Remote Respiration Rate Determination in Video Data
Vital Parameter Extraction based on Optical Flow and Principal Component Analysis

Christian Wiede, Julia Richter, Manu Manuel and Gangolf Hirtz
Department of Electrical Engineering and Information Technology,
Chemnitz University of Technology, Reichenhainer Str. 70, 09126 Chemnitz, Germany

Keywords: Remote Respiration Rate Determination, Vital Parameters, Optical Flow, Principal Component Analysis.

Abstract: Due to the steadily ageing society, the determination of vital parameters, such as the respiration rate, has come into focus of research in recent years. The respiration rate is an essential parameter to monitor a person's health status. This study presents a robust method to remotely determine a person's respiration rate with an RGB camera. In our approach, we detected four subregions on a person's chest, tracked features over time with optical flow, applied a principal component analysis (PCA) and several frequency determination techniques. Furthermore, this method was evaluated in various recorded scenarios. Overall, the results show that this method is applicable in the field Ambient Assisted Living (AAL).

1 INTRODUCTION

Europe, in particular Germany, is facing the problem of a steadily ageing society. According to the national German statistical agency, 29 % of the population will be older than 65 years in 2030 (Statistisches Bundesamt, 2015). Moreover, there will be a lack of medical personnel to care for the elderly. This development goes hand in hand with a higher demand for technical assistance systems, which can support elderly people in their self-determined living.

Current technical assistance systems can either detect emergencies such as falls (Wohlrab et al., 2015) or monitor the daily activities of elderly people (Meinel et al., 2015). Heretofore, these systems cannot monitor a person's current health status, which is one essential requirement to stay longer in the own flat and living in a self-determined way at the same time. This issue could be solved by detecting and tracking vital parameters. These vital parameters, such as heart rate, respiration rate and oxygen saturation, can be measured by means of RGB cameras. In this work, we focus on determining a person's respiration rate accurately and robustly. For this, we propose an algorithm that detects multiple feature points in a region of interest (ROI) at the chest and tracks these points with a Kanade-Lucas-Tomasi (KLT) point tracker (Tomasi and Kanade, 1991). This step is followed by a temporal filtering, a PCA and a frequency determination. Moreover, we proved the reliability for various scenarios in our experiments.

The presented approach has the crucial advantage that it works contact-less. This will be more comfortable for future users, because they are not required to wear additional devices. Moreover, this approach allows the determination of the respiration rate at home in the first place. The respiration rate as vital parameter can provide information about the general current health status and miscellaneous abnormal respiration patterns, which can be indicators for pulmonary diseases. For example, it is possible to detect a sudden breathlessness and inform an emergency doctor immediately, who can react earlier than nowadays. This can save lives and prevent restrictions induced by secondary diseases, which could then be preventable as well. Besides the field of AAL, there exist further possible applications, such as the prevention of sudden infant death syndrome at neonatals at an early stage, sleep monitoring and the tracking of a driver's well being.

This study is structured as follows: In Section 2, a survey about the existing literature is conducted. This is followed by Section 3, where the proposed method is described in detail. Based on this, an experimental study for multiple scenarios is performed in Section 4. This is accompanied by a detailed discussion. Finally, the findings are condensed and future work is outlined.

Wiede C., Richter J., Manuel M. and Hirtz G.
Remote Respiration Rate Determination in Video Data - Vital Parameter Extraction based on Optical Flow and Principal Component Analysis.
DOI: 10.5220/0006095003260333
In *Proceedings of the 12th International Joint Conference on Computer Vision, Imaging and Computer Graphics Theory and Applications (VISIGRAPP 2017)*, pages 326-333
ISBN: 978-989-758-225-7

2 RELATED WORK

The determination of vital parameters is a relevant field in medicine, which has been studied for centuries. Beside the heart rate, the respiration rate indicates a person's individual health state and is therefore suited to assess the personal well-being. Furthermore, a pathologically varied respiration rate, which occurs during breathlessness or hyperventilation, can be a symptom for multiple diseases.

In the clinical environment, there are multiple possibilities to measure the respiration rate, for example respiratory effort belts, nasal thermistors, pressure transducers or by taking the modulated signal of the electrocardiography (ECG). All these established methods have in common the disadvantage that they need direct body contact. These measurement methods cause a large discomfort for elderly people. Therefore, optical methods can contribute to a higher comfort due to their contact-less working mode.

Fei and Pavlidis applied a face and nostrils recognition on thermal images and used a wavelet analysis to determine the thermal change at the nostrils during inhalation and exhalation (Jin Fei and Pavlidis, 2010). Other researchers have chosen the Kinect device for respiration rate detection to monitor the movement of the chest during the breathing. Martinetz et al. tracked the Kinect infra-red pattern over time, applied a PCA and auto regressive (AR) methods to determine the frequency (Martinez and Stiefelhagen, 2012). In contrast to that, Lim et al. used a moving average filter and a spline interpolation on the depth points (Lim et al., 2014). Ostadabbas et al. extended this idea by automatically selecting an ROI on the chest and by measuring depth changes (Ostadabbas et al., 2015).

While all these approaches used different wavelengths in the infra-red spectrum, we want to focus on the visible light spectrum, i. e. by using RGB cameras. In general, the lifting and lowering of the torso and the abdomen could be observed in all existing approaches that determined the respiration rate. Tan et al. proposed to measure the motion by subtracting two consecutive frames and detecting edges (Tan et al., 2010). In comparison to that, Bartula et al. created 1D-profiles of a person and correlated these 1D-vectors of adjacent frames to determine the respiration rate (Bartula et al., 2013). An alternative approach consist of the detection of intensity changes on the skin and the application of an independent component analysis (ICA) to determine the heart rate (Poh et al., 2011). The respiration rate can be determined by a modulation of the heart rate signal. Tarassenko et al. expanded this concept by using AR models for the frequency determination (Tarassenko et al., 2014). In 2015, Sharma et al. used the Eulerian Video Magnification presented by Wu et al. (Wu et al., 2012) to determine the respiration rate by means of intensity changes (Sharma et al., 2015).

Another large group of approaches are tracking based and optical flow based methods. The basics were investigated by Nakajima et al. (Nakajima et al., 2001) and Frigola et al. (Frigola et al., 2002), who used the methods of Horn-Schunck (Horn and Schunck, 1981) or (Pentland and Horowitz, 1991) respectively. Based on this, Lukac et al. use a KLT tracker (Tomasi and Kanade, 1991) for the optical flow (Lukac et al., 2014). This principle was improved by Koolen et al., who applied a PCA, an ICA and a Short Time Fourier Transform (STFT) for signal analysis (Koolen et al., 2015). In the application field of remote heart rate determination, Balakrishnan et al. suggested to firstly find features in the face and then use a point tracker to extract the trajectories (Balakrishnan, 2014). Subsequently, they applied a PCA and determined the heart rate. Li et al. adapted this approach and used it to detect points on the chest for respiration rate determination (Li et al., 2014).

The extant literature revealed that it is possible to extract the human respiration rate with an RGB camera remotely. However, there exist different solutions to reach this aim. We combined several of such solutions to design an accurate and robust system for remote respiration rate detection. Furthermore, we evaluated the proposed algorithm under various conditions.

3 METHODS

3.1 Overview

In the following section, the implemented methods to remotely obtain the respiration rate are presented. The principal steps are visualised in Figure 1. In the first place, images were acquired from an RGB camera. This was followed by an ROI selection on the chest, a feature detection in this ROI and the tracking of these features. The trajectories of the tracked points were extracted and bandpass filtered. Afterwards, a PCA, a channel selection and a frequency determination were performed. This chain outputs the final respiration rate.

3.2 ROI Selection

For the proposed approach, it is necessary to observe the chest or a part of the chest to monitor the lifting and the lowering of the torso, which is induced by the

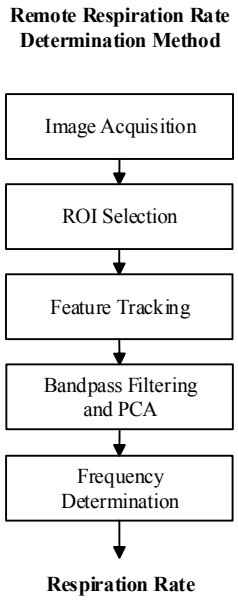

Figure 1: Block diagram of the proposed remote respiration rate determination algorithm.

breathing. There are two possibilities to obtain a stable region of interest on the chest. On the one hand, there is the face detection. By concluding from the position of the face bounding box, the chest bounding box could be estimated. On the other hand, there is the the upper body detection. In this case, the chest bounding box was selected as a part within the upper body bounding box. Both possibilities use a Viola-Jones detector (Viola and Jones, 2004). While the face detector is more accurate, the upper body detector can be applied if the face is not visible, e. g. when the person is not facing the cameras.

In the first place, we applied the face detector. The ROI was placed centrally below the face bounding box by 125 % of the face bounding box height. The height of this ROI is 60 % of the face bounding box height and its width is 120 % of the bounding box width.

If no face could be detected, the upper body detector was applied. The corresponding bounding box height is 20 % of the upper body bounding box height and its width is 36 % to obtain an ROI of the chest. The center is shifted in vertical direction centrally by 65 % of the height of the upper body bounding box.

Finally, the ROI was split in four equally sized quarters, see Figure 2. The advantage of splitting the ROI is a higher robustness of the further processing steps. Noise that effects only one part of the ROIs could be reduced or eliminated in this way.

Figure 2: Proband with the chest bounding box consisting of four subregions and the tracked points.

3.3 Feature Tracking

Before the tracking could be applied, a preliminary feature detection was necessary to identify unique image parts. For this purpose, we used minimum eigenvalue feature (Shi and Tomasi, 1993) in each of the four subregions. Possible corner points were identified by a minimum eigenvalue metric. In Figure 2, the detected features are shown. In order to limit the number of features, only the fifteen strongest points per region were selected.

Based on this, we applied a so-called KLT tracker (Tomasi and Kanade, 1991), which is the base for the optical flow as well. According to the brightness assumption, the intensity of a pixel $I(x,y,t_0)$ at the time t_0 will remain stable over short time durations and small movements. For a single time step dt, the following equation is valid:

$$I(x,y,t_0) = I(x+dx, y+dy, t_0+dt) \tag{1}$$

dx and dy denote the small displacements in x and y direction. Obviously, this equation with two unknown variables cannot be solved. To overcome this issue, Tomasi and Kanade suggested to use the neighbouring pixels as well, since they perform all the same trajectory for a small movement. A 3×3 patch results in nine equations for two unknown variables. This over-determined equation system can be solved by a least square fitting method.

As a result, the trajectories of the n feature points in one subregion were observed in x and y direction:

$$y_n^1(t);\ x_n^1(t) \tag{2a}$$
$$y_n^2(t);\ x_n^2(t) \tag{2b}$$
$$y_n^3(t);\ x_n^3(t) \tag{2c}$$
$$y_n^4(t);\ x_n^4(t) \tag{2d}$$

In the following processing, only the y coordinates were considered, because the principal component of the chest motion during the breathing is the y direction. The mean value Y_{avg} of all feature points in y direction can be considered as the motion of the whole subregion, see Equation 3.

$$Y^1_{\text{avg}}(t) = \frac{1}{n}\sum_i^n y^1_n(t) \tag{3a}$$

$$Y^2_{\text{avg}}(t) = \frac{1}{n}\sum_i^n y^2_n(t) \tag{3b}$$

$$Y^3_{\text{avg}}(t) = \frac{1}{n}\sum_i^n y^3_n(t) \tag{3c}$$

$$Y^4_{\text{avg}}(t) = \frac{1}{n}\sum_i^n y^4_n(t) \tag{3d}$$

If no feature points were found in one subregion, the final signal was substituted by the subregion with the highest number of features. This procedure guarantees a robust processing even if there are no feature points in one subregion.

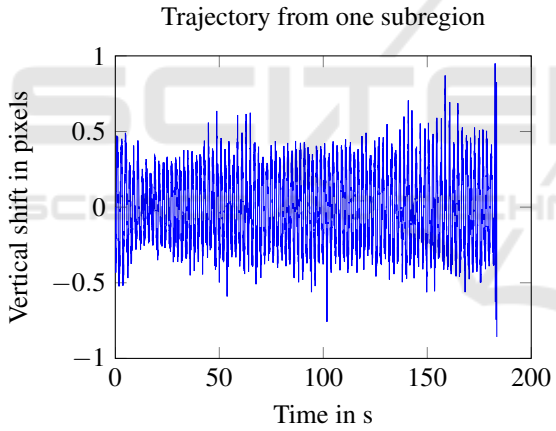

Figure 3: Raw signal of the trajectory of one subregion.

3.4 Bandpass Filtering and PCA

In order to exclude implausible frequencies, which do not lie in the physiological range of the human respiration rate, a bandpass filter BP was applied to all four subregions. An FIR filter with 128 filter coefficients was selected to guarantee a constant group delay. The designed filter allows all frequencies between 0.125 Hz (7.5 BPM) and 0.7 Hz (42 BPM) to pass. This range complies with the natural human respiration rate. Y_{BP} denotes the filtered signal, see Equation 4.

$$Y^1_{\text{BP}}(t) = BP(t) * Y^1_{\text{avg}}(t) \tag{4a}$$

$$Y^2_{\text{BP}}(t) = BP(t) * Y^2_{\text{avg}}(t) \tag{4b}$$

$$Y^3_{\text{BP}}(t) = BP(t) * Y^3_{\text{avg}}(t) \tag{4c}$$

$$Y^4_{\text{BP}}(t) = BP(t) * Y^4_{\text{avg}}(t) \tag{4d}$$

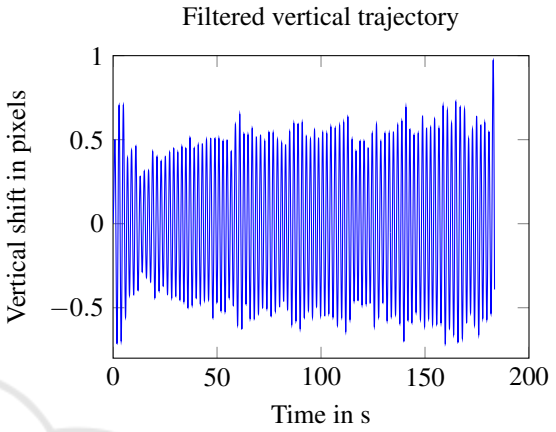

Figure 4: Filtered signal of the trajectory of one subregion.

These filtered signals contain the information of all vertical motions in the assigned frequency range. However, there is still motion present in these signals, which cannot be referred to as breathing. In order to split the bandpass filtered signals in the respiration rate signal and noise signals, we applied a PCA, according to Equation 5. This method detects the principal components in a new orthogonal coordinate system.

$$PC(t) = \text{PCA}(Y^1_{\text{BP}}(t); \ldots; Y^4_{\text{BP}}(t)) \tag{5}$$

In this equation, PC denotes one principal component. In total, there are four resulting principal components. The first principal component is shown in Figure 5. For the subsequent frequency determination, the principal component with the highest spectrum density was selected. In our experiments, the principal component with the highest spectrum density was always the first component.

3.5 Frequency Determination

In this study, we implemented three different methods for frequency determination: the FFT, the spectral estimator described by Welch and a peak counting method. A sliding window of 30 seconds was used for all three methods.

For a specific time t_0, the three methods can be

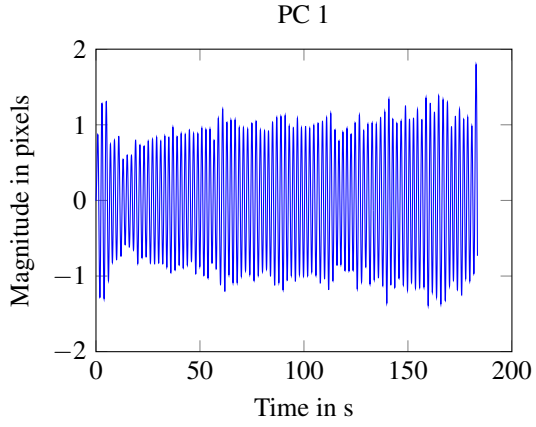

Figure 5: First principal component.

defined as:

$$F_{\text{FFT}}(t_0) = \max(|\text{FFT}(PC)|) \quad (6a)$$

$$F_{\text{Welch}}(t_0) = \max(|\text{Welch}(PC)|) \quad (6b)$$

$$F_{\text{Peaks}}(t_0) = \frac{1}{n_{peaks}} \sum_{t_0}^{t_0+30s} \frac{1}{t_{peak} - t_{peak-1}}, \quad (6c)$$

whereas F_{FFT}, F_{Welch} and F_{Peaks} are the determined respiration rates.

In Figure 6, these respiration rates are displayed over time.

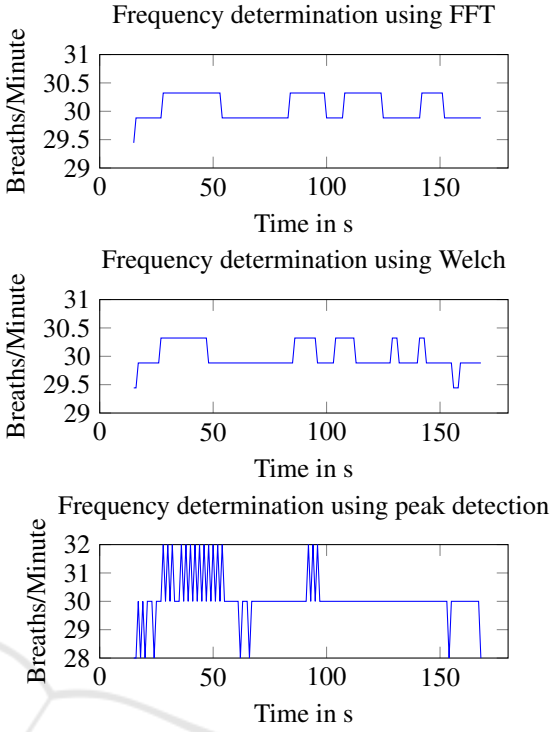

Figure 6: Outputs of the three frequency determination methods: F_{FFT}, F_{Welch} and F_{Peaks}. In this case, the determined respiration rate is approximately 30 breaths per second.

4 RESULTS AND DISCUSSION

4.1 Setting

In order to test the proposed algorithm under various conditions, we created a database of 35 different videos in total. These videos were recorded using an RGB camera, i. e. a Basler acA640-100gc with a resolution of 658×492 pixel. The automatic exposure time control and the automatic white balancing were disabled in order to avoid influences on our measurements. We recorded the videos with a fixed frame rate of 30 frames per second. Each video has a duration of approximately three minutes. In total, five probands took part in our experiments. For the records, no other light sources than daylight or normal ceiling light were used.

For the evaluation, we considered the distance from the camera, the brightness of the image, the influence of different clothing and the orientation of the probands. The considered scenarios are summarised in Table 1. These scenarios will be discussed in the following sections in detail. The scenario with a distant of three metres from the camera, good lighting conditions and with a textured shirt was defined as ideal.

Table 1: Evaluated scenarios in our experiments.

Evaluation criterion	Scenario
Distance	1 m
	3 m
	5 m
Illumination	Good
	Insufficient
Clothing influence	Textured shirt
	Plain shirt
	Extra jacket
View	Back view

For evaluation, we used a set of pre-defined respiration rates as ground truth data. For this, the probands performed guided breathing patterns. That means that they had to breath in a certain fixed breathing frequency to approximately reach the defined ground truth value. Defined ground truth values were 30 BPM, 25 BPM, 20 BPM, 15 BPM and 7.5 BPM. This results in a maximal possible error resolution of 3.75 BPM. The breathing patterns were randomly chosen for different probands and sequences. In or-

der to compare the determined respiration rate with the ground truth, we assigned this determined respiration rate to the nearest value of the defined breathing pattern values. Then, we evaluated whether this assigned value is equal to the ground truth value of the sequence or not.

4.2 Distance from Camera

One essential criterion for a robust algorithm is the invariance against scaling. The respiration rate determination should not be depended on the distance between the camera and a person. For evaluation, three different distances to the camera were chosen, i. e. 1 m, 3 m and 5 m. Five videos were recorded for each scenario, which results in quantisation steps of 20 % for five probands. All three frequency determination measurement methods were applied.

Table 2: Classification rates for the distance scenarios.

Distance	FFT	Welch	Peak
1 m	100 %	100 %	100 %
3 m	100 %	100 %	100 %
5 m	100 %	100 %	80 %

As shown in Table 2, the distance does not substantially influence the proposed algorithm. The algorithm fails to determine the correct respiration rate only for one proband at a distance of five metres for the peak detection. This person's chest was partially covered by long hair falling from the head. Nonetheless, the respiration rate for the other videos could be successfully determined for this person. Hence, it can be concluded that the algorithm is scale-invariant as long as there are still features available.

4.3 Illumination

The lighting condition in a room can change very quickly, for example when ceiling lights are switched on or off or the incoming sunlight changes its intensity due to clouds. In these scenarios, the proposed algorithm should continuously track the features without loosing too many features. In our first setting, we recorded the five probands under perfect lighting conditions. Then, in the second setting, the ceiling lights were switched off, so that the illumination and the contrast were low in this setting.

Table 3: Classification rates for the illumination scenarios.

Illumination	FFT	Welch	Peak
Good	100 %	100 %	100 %
Insufficient	100 %	100 %	100 %

The proposed method managed both good illumination conditions and insufficient illumination, see Table 3. The respiration rate was detected in all videos and with all probands for this scenario. It can be concluded that the illumination does not have a substantial effect on the algorithm output.

4.4 Influence of Clothing

Another major influence factor consists in the type of clothing that is worn. Since the proposed method is feature-based, the texture of the shirt plays an important role. In the standard case, a shirt with patterns (texture) was used. In contrast to that, in the second case, the probands wore a blank shirt with a homogeneous appearance. We expected that less or no features would be found in the subregions. In a third case, the probands wore an additional jacket. Due to the fact that there is partially air between the shirt and the jacket, the breathing patterns might not be transferred to the jacket.

Table 4: Classification rates for the clothing scenarios.

Clothing	FFT	Welch	Peak
Textured shirt	100 %	100 %	100 %
Plain shirt	100 %	100 %	100 %
Extra jacket	100 %	100 %	100 %

In all three scenarios, the correct respiration rates were estimated for all probands, see Table 4. Despite the decreased number of features in the four subregions for the blank shirt, a sufficient number of features was still detectable. These features appeared especially at the collar or buttons of the shirt. Additionally, it can be observed that the respiration rate could be determined even when the probands wore a jacket. That means that the transfer of the breathing motion was still large enough to accurately determine the respiration rate.

4.5 Back View

In real scenarios, it is not guaranteed that a person is always looking frontal at the camera. For that reason, all probands' back views were recorded for one scenario.

Table 5: Classification rates for the back view.

View	FFT	Welch	Peak
Back view	100 %	100 %	80 %

As shown in Table 5, the peak detection algorithm failed to detect the correct respiration rate for only one proband. This, again, can be explained with the

proband's long hair, which covered the back of the upper body. The FFT and the Welch estimation method were still able to predict the correct respiration rate.

4.6 Overall Comparison

Overall, 35 videos were considered for the testing. In general, in all scenarios the respiration rate could be classified correctly, see Table 6. While the peak detection method was able to detect the correct respiration rate only in 94.4 % of the cases, the FFT and the Welch spectral estimation worked perfectly for all scenarios. Therefore, it is recommended to use one of those two methods to determine the frequency for the respiration rate.

Table 6: Overall classification rates.

Method	FFT	Welch	Peak
Overall	100 %	100 %	94.4 %

5 CONCLUSION AND FUTURE WORK

In this study, we developed a new method for remote respiration rate determination, which is based on four ROIs, an optical flow based tracking, a PCA and a frequency determination. Furthermore, an intense evaluation of different environmental parameters and scenarios was conducted. The results show that the presented method worked robustly in all scenarios. The best frequency determination methods were the FFT and the Welch spectral estimation. The results reveal that it is possible to use such a respiration rate estimation system in a domestic environment for AAL. Further studies have to evaluate whether the accuracy is sufficient for clinical use.

For future work, the influence of motion has to be evaluated. If the respiration rate and the superimposed motion signal could be separated, this method could be used as well in the field of e-rehabilitation or in professional sports. Moreover, we intend to develop a real-time working system to detect the respiration rate immediately.

ACKNOWLEDGEMENTS

This project is funded by the European Social Fund (ESF). We furthermore would like to express our thanks to all the persons who contributed to this project with their recordings.

REFERENCES

Balakrishnan, G. (2014). *Analyzing pulse from head motions in video*. PhD thesis, Massachusetts Institute of Technology.

Bartula, M., Tigges, T., and Muehlsteff, J. (2013). Camera-based system for contactless monitoring of respiration. In *Engineering in Medicine and Biology Society (EMBC), 2013 35th Annual International Conference of the IEEE*, pages 2672–2675. IEEE.

Frigola, M., Amat, J., and Pags, J. (2002). Vision based respiratory monitoring system. In *Proceedings of the 10th Mediterranean Conference on Control and AutomationMED2002 Lisbon, Portugal*.

Horn, B. K. and Schunck, B. G. (1981). Determining optical flow. *Artificial intelligence*, 17(1-3):185–203.

Jin Fei and Pavlidis, I. (2010). Thermistor at a Distance: Unobtrusive Measurement of Breathing. *IEEE Transactions on Biomedical Engineering*, 57(4):988–998.

Koolen, N., Decroupet, O., Dereymaeker, A., Jansen, K., Vervisch, J., Matic, V., Vanrumste, B., Naulaers, G., Van Huffel, S., and De Vos, M. (2015). Automated Respiration Detection from Neonatal Video Data:. In *Proceedings of the International Conference on Pattern Recognition Applications and Methods*, pages 164–169. SCITEPRESS - Science and and Technology Publications.

Li, M. H., Yadollahi, A., and Taati, B. (2014). A non-contact vision-based system for respiratory rate estimation. In *Engineering in Medicine and Biology Society (EMBC), 2014 36th Annual International Conference of the IEEE*, pages 2119–2122. IEEE.

Lim, S. H., Golkar, E., Rahni, A., and Ashrani, A. (2014). Respiratory motion tracking using the kinect camera. In *Biomedical Engineering and Sciences (IECBES), 2014 IEEE Conference on*, pages 797–800. IEEE.

Lukac, T., Pucik, J., and Chrenko, L. (2014). Contactless recognition of respiration phases using web camera. In *Radioelektronika (RADIOELEKTRONIKA), 2014 24th International Conference*, pages 1–4. IEEE.

Martinez, M. and Stiefelhagen, R. (2012). Breath rate monitoring during sleep using near-ir imagery and pca. In *Pattern Recognition (ICPR), 2012 21st International Conference on*, pages 3472–3475. IEEE.

Meinel, L., Richter, J., Schmidt, R., Findeisen, M., and Hirtz, G. (2015). Opdemiva: An integrated assistance and information system for elderly with dementia. In *Consumer Electronics (ICCE), 2015 IEEE International Conference on*, pages 76–77.

Nakajima, K., Matsumoto, Y., and Tamura, T. (2001). Development of real-time image sequence analysis for evaluating posture change and respiratory rate of a subject in bed. *Physiological Measurement*, 22(3):N21.

Ostadabbas, S., Sebkhi, N., Zhang, M., Rahim, S., Anderson, L. J., Lee, F. E.-H., and Ghovanloo, M. (2015). A Vision-Based Respiration Monitoring System for Passive Airway Resistance Estimation. *IEEE Transactions on Biomedical Engineering*, pages 1–1.

Pentland, A. and Horowitz, B. (1991). Recovery of nonrigid motion and structure. *IEEE Transactions on Pattern Analysis and Machine Intelligence*, 13(7):730–742.

Poh, M.-Z., McDuff, D., and Picard, R. (2011). Advancements in Noncontact, Multiparameter Physiological Measurements Using a Webcam. *Biomedical Engineering, IEEE Transactions on*, 58(1):7–11.

Sharma, S., Bhattacharyya, S., Mukherjee, J., Purkait, P. K., Biswas, A., and Deb, A. K. (2015). Automated detection of newborn sleep apnea using video monitoring system. In *Advances in Pattern Recognition (ICAPR), 2015 Eighth International Conference on*, pages 1–6. IEEE.

Shi, J. and Tomasi, C. (1993). Good Features to Track. Technical report, Cornell University, Ithaca, NY, USA.

Statistisches Bundesamt (2015). 13. koordinierte Bevöelkerungsvorausberechnung für Deutschland. https://www.destatis.de/bevoelkerungspyramide/. [Online; accessed 07-Septemper-2016].

Tan, K. S., Saatchi, R., Elphick, H., and Burke, D. (2010). Real-time vision based respiration monitoring system. In *Communication Systems Networks and Digital Signal Processing (CSNDSP), 2010 7th International Symposium on*, pages 770–774. IEEE.

Tarassenko, L., Villarroel, M., Guazzi, A., Jorge, J., Clifton, D. A., and Pugh, C. (2014). Non-contact video-based vital sign monitoring using ambient light and auto-regressive models. *Physiological Measurement*, 35(5):807–831.

Tomasi, C. and Kanade, T. (1991). Detection and Tracking of Point Features. Technical report, Carnegie Mellon University.

Viola, P. and Jones, M. J. (2004). Robust real-time face detection. *International Journal of Computer Vision*, 57(2):137–154.

Wohlrab, D., Heß, M., Apitzsch, A., Langklotz, M., Schwarzenberger, A., Bilda, S., Schulz, H., Hirtz, G., and Mehner, J. (2015). Hom-e-call - an enhanced fall detection system based on accelerometer and optical sensors applicable in domestic environment. In Jaffray, D. A., editor, *World Congress on Medical Physics and Biomedical Engineering, June 7-12, 2015, Toronto, Canada*, volume 51 of *IFMBE Proceedings*, pages 1461–1464. Springer International Publishing.

Wu, H.-Y., Rubinstein, M., Shih, E., Guttag, J., Durand, F., and Freeman, W. T. (2012). Eulerian Video Magnification for Revealing Subtle Changes in the World. *ACM Trans. Graph. (Proceedings SIGGRAPH 2012)*, 31(4).